

Ground state of the Bethe lattice spin glass and running time of an exact optimization algorithm

Frauke Liers,^{1,*} Matteo Palassini,^{2,†} Alexander K. Hartmann,^{3,‡} and Michael Jünger^{1,§}

¹Universität zu Köln, Institut für Informatik, Pohligstraße 1, 50969 Köln, Germany

²University of California San Francisco, 3333 California Street, Suite 415, San Francisco, CA 94118, USA

³Institut für Theoretische Physik, Universität Göttingen, Bunsenstr. 9, 37073 Göttingen, Germany

(Dated: February 23, 2019)

We study the Ising spin glass on random graphs with fixed connectivity z and with a Gaussian distribution of the couplings, with mean μ and unit variance. We compute exact ground states by using a sophisticated branch-and-cut method for $z = 4, 6$ and system sizes up to 1280 spins, for different values of μ . We locate the spin-glass/ferromagnet phase transition at $\mu = 0.77 \pm 0.02$ ($z = 4$) and $\mu = 0.56 \pm 0.02$ ($z = 6$). We also compute the energy and magnetization in the Bethe-Peierls approximation with a stochastic method, and estimate the magnitude of replica symmetry breaking corrections. Near the phase transition, we observe a sharp change of the median running time of our implementation of the algorithm, consistent with a change from a polynomial dependence on the system size, deep in the ferromagnetic phase, to slower than polynomial in the spin-glass phase.

I. INTRODUCTION

Recent years have seen an increasing interaction between the fields of combinatorial optimization and statistical physics^{1,2,3}. On one hand, several problems in the statistical physics of disordered systems have been mapped onto combinatorial problems, for which fast combinatorial optimization algorithms are available^{4,5}. This has provided valuable insights into questions that are hard to investigate with traditional techniques, such as Monte Carlo simulations. On the other hand, concepts and methods from statistical physics are increasingly applied to combinatorial optimization.

Easy/hard thresholds analogous to phase transitions have been observed in random instances of optimization and decision problems, including satisfiability (SAT)^{6,7}, vertex-cover⁸ (VC), number partitioning⁹, and others. There is currently much interest in understanding how phase transitions affect the performance of combinatorial algorithms, following the observation¹⁰ that the *average*¹¹ or *typical* (i.e. median) running time of some algorithms exhibits a sharp change in the vicinity of a phase transition. For example, in 3SAT, a special case of SAT, and in VC, the typical running time of exact backtracking algorithms changes^{12,13} from a polynomial dependence on the input size (in the "solvable" region) to exponential dependence (in the "unsolvable" region). This provides an insight into the performance of algorithms that goes beyond the *worst-case* running time usually considered in the analysis of algorithms. Recently, statistical physics techniques have been fruitfully applied to study combinatorial problems and the behavior of optimization algorithms³.

In this paper, we apply a branch-and-cut algorithm, a technique developed in combinatorial optimization, to find the ground state of the Ising spin glass on random graphs with fixed coordination number (also called Bethe lattices).

Our motivation is twofold. The first goal is algo-

rithmic: we want to characterize the typical running time of our algorithm, notably its behavior across the zero-temperature spin-glass/ferromagnet phase transition that occurs when varying the mean of the random couplings. The interest stems from the importance of branch-and-cut as a general technique in combinatorial optimization. Furthermore, finding the ground state of a spin glass is a prominent example of a hard optimization problem arising from statistical physics (in general, it is *NP-hard*¹⁴, see Section III). The performance of branch-and-cut for this application has not been investigated in detail before (see, however, Refs. 15, 16 and 17), and here we fill this gap. Unlike in SAT, VC and other classical combinatorial problems, here averaging over random instances is physically motivated. To our knowledge, the only other study relating a "physical" phase transition to algorithmic performance is that of Middleton¹⁸, which investigates the typical running time of the matching algorithm for the random-field Ising model, which however is polynomial everywhere in the parameter space.

The second motivation for the present work lies in the ground state properties of the Bethe lattice spin glass, which recently have attracted a renewed interest^{19,20,21,22}. Using branch-and-cut, we compute the ground state energy and magnetization, and locate the spin-glass/ferromagnet phase transition. This provides a useful test of recently developed analytical methods to treat diluted spin glass models^{19,20,23}. In particular, we solve the model in the Bethe-Peierls (BP) approximation (equivalent to the replica symmetric approximation in the replica formalism) using a stochastic approach as in Refs. 20,24.

We find that the median running time of our algorithm varies sharply near the spin-glass/ferromagnet transition, indicating a change from polynomial time (deep in the ferromagnetic phase) to slower than polynomial (in the spin glass phase). We also observed a similar behavior for spin glasses on regular lattices in two and three dimensions (not reported here). Note that the running time of

one special algorithm, strictly speaking, does not allow us to draw conclusions about the “hardness” of the problem itself. By comparing the branch-and-cut results with the results in the BP approximation, we estimate the magnitude of the replica symmetry breaking corrections to the ground state energy and magnetization, finding that they are small.

The rest of the paper is organized as follows. In Section II, we introduce the Bethe lattice spin glass model. In Section III, we describe the branch-and-cut algorithm used to calculate the exact ground states of the model. In Section IV, we describe the Bethe-Peierls approximation and the stochastic procedure used to solve it. In Section V, we present our branch-and-cut and BP results for the ground state energy and the zero temperature phase transition. In Section VI, we show that this transition coincides with a change of the typical running time. Finally, Section VII summarizes our results.

II. MODEL

The system considered consists of N Ising spins $S_i = \pm 1$ sitting on the nodes of a graph $G = (V, E)$, where $V = \{1, \dots, N\}$ is the set of nodes and $E = \{(i, j)\} \subset V \times V$ is the set of edges of the graph. The energy of the system is given by

$$\mathcal{H} = - \sum_{(i,j) \in E} J_{ij} S_i S_j \quad (1)$$

where the couplings J_{ij} are distributed according to a Gaussian distribution with mean μ and unit variance.

We consider the case in which G is a random graph with fixed connectivity z , or z -regular graph, where each spin interacts with exactly z neighbors. This provides a convenient realization of a Bethe lattice, which avoids some complications associated to the usual construction of a Bethe lattice from a Cayley tree¹⁹. Frustration is induced by large loops, the typical size of a loop being of order $\log(N)$. Small loops are rare, giving the graph a local tree-like structure, and therefore the mean field approximation is exact. A related model is the Viana-Bray model²⁵, in which the connectivity is a Poisson variable with finite mean. Finite-connectivity or “diluted” models provide a better approximation to finite-dimensional spin glasses than the infinitely-connected Sherrington-Kirkpatrick model. Furthermore, they are directly related to optimization problems such as graph partitioning and coloring.

Although it has long been known that replica symmetry is broken in these two models^{25,26,27}, until recently a replica symmetry broken solution could be found only in some limit cases. Mézard and Parisi recently introduced^{19,20} a “population dynamics” algorithm which allows a full numerical solution at the level of one step of replica symmetry breaking. Explicit results were derived for the Bethe lattice spin glass with the $\pm J$

disorder distribution, but not for the Gaussian distribution considered here. Previous numerical studies of this model can be found in Refs. 22,28,29. For a complete discussion of the Bethe lattice spin glass, see Ref. 19 and references therein.

III. BRANCH-AND-CUT ALGORITHM

The problem of finding a ground state of the Hamiltonian in Eq. (1) is in general computationally very demanding. For a generic graph G , it is NP-hard^{5,14}. For NP-hard problems, currently only algorithms are available, for which the running time increases faster than any polynomial in the system size, in the worst case (see Section VI for a brief description of complexity classes). In the special case of a planar system without magnetic field, e.g. a square lattice with periodic boundary conditions in at most one direction, efficient polynomial-time matching algorithms³⁰ exist. For the square lattice with periodic boundaries in *both* directions, polynomial algorithms exist for computing the complete partition function for the $\pm J$ distribution³¹ and for the case in which the coupling strengths are bounded by a polynomial in the system size³². In practice, both algorithms can only reach relatively small system sizes.

For the Bethe lattice considered here (and for regular lattices in dimension higher than two), no polynomial algorithm is known. Heuristic algorithms recently used include simulated annealing³³, “multicanonical” simulation³⁴, genetic algorithms^{35,36}, extremal optimization²², a hierarchical renormalization-group based approach³⁷, and the cluster-exact approximation algorithm³⁸. Here, however, we are interested in investigating the running time of an exact, deterministic algorithm, since in this case the running time to find the exact ground state is a well defined quantity. We study the branch-and-cut method^{15,39} (see Ref. 40 for a tutorial on optimization problems and techniques, including branch-and-bound and branch-and-cut), which is currently the fastest exact algorithm for computing spin glass ground states¹⁷, with the exception of the polynomial-time special cases mentioned above. As the branch-and-cut method is basically branch-and-bound with cutting planes, we also did some experiments with a pure branch-and-bound algorithm^{41,42}, which however can only deal with much smaller system sizes. We found that the running time behaves in a qualitatively similar but less clear way to branch-and-cut, in the accessible range of sizes.

In the rest of this Section, we repeat a short description of the branch-and-cut method already given in Ref. 17, to the benefit of the reader. It is convenient to map the problem of minimizing the Hamiltonian in Eq.(1) into a *maximum cut* problem. Consider a graph $G = (V, E)$, and let assign weights $\{K_{ij}\}$ to the edges. Given a partition of the node set V into a subset $W \subset V$ and its complement $V \setminus W$, the *cut* $\delta(W)$ associated to W is the set

of edges with one endpoint in W and the other endpoint in $V \setminus W$, namely $\delta(W) = \{(ij) \in E \mid i \in W, j \in V \setminus W\}$. The *weight* of $\delta(W)$ is defined as the sum of the weights of the cut edges, $\sum_{(ij) \in \delta(W)} K_{ij}$. The *maximum cut* is a node partition with maximum weight among all partitions. It can be shown³⁹ that minimizing the Hamiltonian in Eq.(1) is equivalent to finding a maximum cut of G with the assignment $K_{ij} = -J_{ij}$.

The branch-and-cut algorithm solves the maximum cut problem through simultaneous lower and upper bound computations. By definition, the weight of any cut gives a *lower bound* on the optimal cut value. Thus, we can start from any cut and iteratively improve the lower bound using deterministic heuristic rules (local search and other specialized heuristics, see Ref. 43 for details). How do we decide when a cut is optimal? This can be done by additionally maintaining *upper bounds* on the value of the maximum cut. Upon iteration of the algorithm, progressively tighter bounds are found, until optimality is reached.

Since the availability of upper bounds marks the difference between a heuristic and an exact solution, we now summarize how the upper bound is computed (for more details, see Ref. 43.) To each edge (ij) we associate a real variable x_{ij} and to each cut $\delta(W)$ an *incidence vector* $\chi^{\delta(W)} \in \mathbb{R}^E$ with components $\chi_{ij}^{\delta(W)}$ associated to each edge (ij) , where $\chi_{ij}^{\delta(W)} = 1$ if $(ij) \in \delta(W)$ and $\chi_{ij}^{\delta(W)} = 0$ otherwise. Denoting by $P_C(G)$ the convex hull of the incidence vectors, it can be shown that a *basic optimum solution*⁴⁴ of the linear program

$$\max \left\{ \sum_{(ij) \in E} J_{ij} x_{ij} \mid x \in P_C(G) \right\}. \quad (2)$$

is a maximum cut. In order to solve (2) with linear programming techniques we would have to express $P_C(G)$ in the form

$$P_C(G) = \{x \in \mathbb{R}^E \mid Ax \leq b, 0 \leq x \leq 1\} \quad (3)$$

for some matrix A and some vector b . Whereas the existence of A and b are theoretically guaranteed, even subsets of $Ax \leq b$ known in the literature contain a huge number of inequalities that render a direct solution of (2) impractical.

Instead, the branch-and-cut algorithm proceeds by optimizing over a *superset* P containing $P_C(G)$, and by iteratively tightening P , generating in this way progressively better upper bounds. The supersets P are generated by a *cutting plane* approach. Starting with some P , we solve the linear program $\max \left\{ \sum_{(ij) \in E} J_{ij} x_{ij} \mid x \in P \right\}$ by Dantzig's simplex algorithm⁴⁴. Optimality is proven if either of two conditions is satisfied: (i) the optimal value equals the lower bound; (ii) the solution vector \bar{x} is the incidence vector of a cut.

If neither is satisfied, we have to tighten P by solving the *separation problem*. This consists in identifying inequalities that are valid for all points in $P_C(G)$, yet are

violated by \bar{x} , or reporting that no such inequality exists. The inequalities found in this way are added to the linear programming formulation, obtaining a new tighter partial system $P' \subset P$ which does not contain \bar{x} . The procedure is then repeated on P' and so on.

At some point, it may happen that (i) and (ii) are not satisfied, yet the separation routines do not find any new cutting plane. In this case, we *branch* on some fractional edge variable x_{ij} (i.e. a variable $x_{ij} \notin \{0, 1\}$), creating two subproblems in which x_{ij} is set to 0 and 1, respectively. We then apply the cutting plane algorithm recursively for both subproblems.

IV. BETHE-PEIERLS APPROXIMATION

We recall here the zero-temperature formulation of the BP approximation, loosely following Ref. 20. We consider the Hamiltonian Eq.(1) on a random graph with fixed connectivity $z = k + 1$, in which however some spins S_i (*cavity* spins) have only k neighbors. The random couplings are drawn from a distribution $P(J)$. The BP approximation consists in assuming that the ground state energy of this system is given by $E = \text{const.} - \sum_i h_i S_i$, where the sum runs over all cavity spins. The cavity fields h_i , implicitly defined by this relation, are independent, identically distributed random variables when considered as a function of the random couplings. Their distribution $P(h)$ is the central object of interest, and satisfies a recursion relation derived as follows. Suppose we add a new spin S_0 to the system, which interacts with k pre-existing cavity spins S_1, \dots, S_k through couplings J_1, \dots, J_k , and we minimize the energy with respect to S_1, \dots, S_k . Now S_0 is a cavity spin, and it follows immediately that its cavity field h_0 is given by

$$h_0 = \sum_{i=1}^k u(J_i, h_i), \quad (4)$$

where $u(J_i, h_i) = \frac{1}{2}(|h_i + J_i| - |h_i - J_i|)$. This provides a recursion relation for $P(h)$ as the J 's fluctuate according to $P(J)$. Given a spin S_0 interacting with $k + 1$ neighbors with couplings J_1, \dots, J_{k+1} , the internal field H acting on S_0 is

$$H = \sum_{i=1}^{k+1} u(J_i, h_i). \quad (5)$$

Therefore, if we know $P(h)$ we can determine the probability distribution $P(H)$, and the BP magnetization

$$m_{BP} = \lim_{\epsilon \rightarrow 0^+} \int dH P(H) \text{sgn}(H), \quad (6)$$

where $\text{sgn}(x)$ is the sign function and ϵ is a small field that breaks the symmetry of Eq.(4) with respect to changing the sign of all cavity fields.

The knowledge of $P(h)$ is also sufficient to determine the ground state energy of the system. As shown in Ref. 20, this can be expressed as

$$e_{BP} = [\Delta E^{(1)}] - \frac{k+1}{2} [\Delta E^{(2)}], \quad (7)$$

where $[\dots]$ is the expectation value with respect to $P(J)$ and $P(h)$, and the quantities $\Delta E^{(1)}, \Delta E^{(2)}$ are given by

$$\Delta E^{(1)} = - \sum_{i=1}^{k+1} a(J_i, h_i) - \left| \sum_{i=1}^{k+1} u(J_i, h_i) \right| \quad (8)$$

and

$$\Delta E^{(2)} = - \max_{S_i, S_j} (h_i S_i + h_j S_j + J_{ij} S_i S_j), \quad (9)$$

where $a(J_i, h_i) = \frac{1}{2}(|h_i + J_i| + |h_i - J_i|)$ and S_i, S_j in Eq.(9) are two randomly chosen cavity spins which we connect with the coupling J_{ij} .

The BP recursion, especially at finite temperature, has been studied extensively (see Ref. 19 and references therein). In particular, Mézard and Parisi²⁰ have given an analytic expression of $P(h)$ for a binary $P(J)$. Klein et al.⁴⁵ solved the finite temperature BP recursion for Gaussian couplings with $\mu = 0$ in the vicinity of the spin-glass/paramagnet transition. No analytical solution has been derived for Gaussian couplings at $T = 0$, to our knowledge, although Klein et al.⁴⁵ derived an analytic solution near the spin-glass/ferromagnet transition $\mu = \mu_c$ within the *mean random field* approximation.

Here, we employed a stochastic iterative procedure proposed by Mézard and Parisi²⁰ for the more general one-step replica symmetry broken case (see also Ref. 27 for a previous application of a similar method). We consider a population of \mathcal{N} sites, to which we associate \mathcal{N} cavity fields, which are initially assigned at random (with a small positive bias). We then select k sites at random, extract k couplings from $P(J)$, compute h_0 from Eq.(4), and assign h_0 as the new cavity field of a randomly chosen site. We iterate this procedure \mathcal{M} times per site. After a certain number of iterations, the distribution $P(h)$ will satisfy Eq.(4). At each iteration, by merging $k+1$ randomly chosen sites we compute the internal field H with Eq.(5), and $\Delta E^{(1)}$ with Eq.(8), and by merging two sites we compute $\Delta E^{(2)}$ with Eq.(9). After discarding the first $\mathcal{M}/4$ iterations, by averaging $\text{sgn}(H)$, $\Delta E^{(1)}$ and $\Delta E^{(2)}$ over the remaining iterations we estimate m_{BP} and e_{BP} , and their statistical error is obtained from a binning procedure. We repeated the procedure for many values of μ , choosing $\mathcal{M} = 10^4$ and \mathcal{N} between 10^3 and 10^5 , the larger population being near the transition point. With the largest population, the procedure requires about one hour of computer time.

We note that the BP approximation is known to be wrong, being equivalent to the replica symmetric solution which is unstable. The iterative procedure of Mézard and Parisi¹⁹, of which the procedure described above is a

particular case, is able to deal with the one-step replica symmetry breaking case. We have not attempted this here since, for the Gaussian case considered, it would require a significant computing time, and since, as we will see, the BP approximation gives sufficiently accurate results for our purposes.

V. RESULTS

We have studied the Ising spin glass on random graphs with fixed connectivity $z = 4$ and $z = 6$. The instance generator first builds a random regular graph with the algorithm described in Ref. 46. We then assign the couplings J_{ij} according to a Gaussian distribution $P(J)$ with mean μ and variance one.

Using the branch-and-cut approach we were able to study graph sizes up to $N = 400$ for $z = 4$ and $\mu \leq 0.9$, and up to $N = 200$ for $z = 6$ and $\mu \leq 0.7$. For larger values of μ , we considered sizes up to $N = 1280$. The ground states for the smallest systems can be obtained within a second, while the longest computations lasted at most one day on a typical workstation. Incidentally, for Ising spin glasses on a regular grid, specialized heuristics exist that exploit the grid structure, making it possible to consider larger system sizes than for the model reported here. More on timing issues, in relation to the spin-glass/ ferromagnet phase transition, is presented in Section VI.

All the results were averaged over many samples (a sample, or instance, is a realization of the random graph with a realization of the couplings). The largest number of samples were considered in the vicinity of the phase transition, where the fluctuations of the magnetization are larger. Near the transition, for sizes $N \leq 240$ ($z = 4$) and $N \leq 160$ ($z = 6$) we computed around 5000 samples for each value of μ ; for $N = 400$ ($z = 4$) and $N = 200$ ($z = 6$), around 500 samples for each value of μ . For sizes larger than these, we computed up to 280 samples for each μ . In the following analysis of the ground state energy and magnetization, we consider only sizes up to $N = 400$ ($z = 4$) and $N = 200$ ($z = 6$), since for larger sizes the statistical error is quite large. In the analysis of running times we will include all sizes.

A. Ground state energy

We start by showing, in Fig. 1, the average ground-state energy $E(\mu, N)$, divided by zN , as a function of μ for $z = 4, 6$ and two different system sizes. For sufficiently large μ , the system is completely magnetized, therefore the ground-state energy depends linearly on μ as $E(\mu, N)/N \propto z\mu$, as visible in the figure. For small μ the system is frustrated, hence the energy saturates. Note that $E(0, N)$ scales as \sqrt{z} , not as z , therefore the two curves diverge at small μ . The lines in Fig. 1 represent the numerical solution of the BP recursion obtained

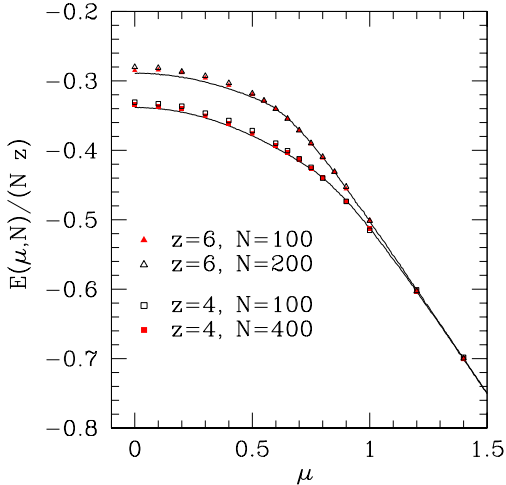


FIG. 1: Average ground state energy, normalized by the number of spins, N , and the connectivity, z , as a function of μ . The symbols represent the numerical results obtained with the branch-and-cut algorithm. The statistical errors, not shown, are smaller than the symbol sizes. The lines represent the numerical solution of the BP recursion. They are obtained by connecting points spaced by $\Delta\mu = 0.005$ ($\Delta\mu = 0.001$ near the transition). The statistical error is comparable to the line thickness.

with a population size $\mathcal{N} = 10^3$ (we verified that with $\mathcal{N} = 10^5$ the results are unchanged) and $\mathcal{M} = 10^4$ iterations of the stochastic algorithm. Clearly, the branch-and-cut results agree well with the BP approximation.

We extrapolate the branch-and-cut results to $N = \infty$ by fitting the data with the form $E/N = e_\infty + bN^{-2/3}$. As shown in Fig. 2, the finite size corrections are well described by a $N^{-2/3}$ dependence for small μ , although an $N^{-\omega}$ correction fits reasonably well the data for other values of ω between 0.6 and 1 as well. For large μ , the finite size corrections are very small. A $N^{-2/3}$ correction was also found to fit well the numerical data by Boettcher²², who computed the average ground state energy of the $\pm J$ model for z up to $z = 26$ and N up to $N = 2048$ using a heuristic algorithm. In Ref. 19, the finite-size dependence of the energy at $T = 0.8$ was studied, for the $\pm J$ distribution and $z = 6$, finding a finite-size exponent $\omega = 0.767(8)$, not far from $2/3$. For the Viana-Bray model with fluctuating connectivity with mean $z = 6$, the value $\omega = 0.62 \pm 0.05$, compatible with $2/3$, was found⁴⁷ also using a heuristic algorithm.

Fig. 2 also shows that the extrapolated energy, e_∞ , is very close to the BP result, e_{BP} , in the whole range of μ . Of course, the agreement is not surprising for large μ , where replica symmetry holds. For smaller μ , the observed agreement indicates that replica symmetry breaking corrections to the ground state energy are small (less than 1%). The same conclusion was reached in Ref. 20 for the $\pm J$ distribution.

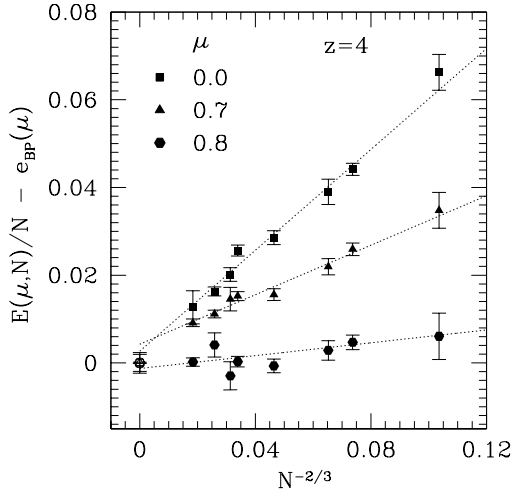


FIG. 2: Size dependence of the ground state energy, for $z = 4$ and $\mu = 0, 0.7$ and 0.8 . The lines represent the best fits with the form $E/N = e_\infty + bN^{-2/3}$. The $N = \infty$ data are the values obtained in the BP approximation.

In particular, for $\mu = 0$ we obtain $e_\infty = -1.38 \pm 0.04$ ($z = 4$) and $e_\infty = -1.72 \pm 0.02$ ($z = 6$), where the errors take into account the uncertainty on the correction exponent ω , to be compared with the BP result $e_{BP} = -1.351 \pm 0.002$ ($z = 4$) and $e_{BP} = -1.737 \pm 0.002$ ($z = 6$). It is also interesting to compare this with the ground-state energy per spin found in two⁴⁸ and three dimensions³⁵ (which have coordination number $z = 4$ and $z = 6$, respectively) with Gaussian couplings and $\mu = 0$, which is $e_\infty = -1.31453(3)$ and $e_\infty = -1.7003(1)$ respectively.

B. Ground state magnetization

In Figs. 3 and 4 we show, for $z = 4$ and 6 respectively, the average ground state magnetization $m = [M]_J$, where $M = \frac{1}{N} \sum_i S_i$ and $[\dots]_J$ denotes the sample average, as a function of μ for different system sizes N . The lines show the $N = \infty$ result in the BP approximation. For small μ , the magnetization vanishes as $1/\sqrt{N}$. For large μ , the finite- N data agree with the BP result within the error bars, with negligible finite-size corrections (again, we recall that the BP approximation is exact for sufficiently large μ). From the point at which the BP magnetization vanishes, we estimate $\mu_c = 0.742 \pm 0.005$ ($z = 4$) and $\mu_c = 0.546 \pm 0.005$ ($z = 6$). Note that recursion relation Eq.(4) admits two symmetric solutions for $\mu > \mu_c$. Hence, in the stochastic procedure the magnetization will oscillate between positive and negative values, with an oscillation “time” (number of iterations) \mathcal{M}_0 that increases with the population size \mathcal{N} and with μ . Therefore, in order to compute the magnetization correctly, we need

$\mathcal{M}_0 \gg \mathcal{M}$. In order to realize this, we increased the size of the population progressively from $\mathcal{N} = 10^3$ to $\mathcal{N} = 10^5$ as μ approached μ_c . Residual oscillations very close to μ_c introduce a small systematic error⁵⁰, which is reflected in the errors for μ_c quoted above.

Another estimate of μ_c can be obtained from the Binder cumulant⁴⁹

$$g(\mu) = \frac{1}{2} \left(3 - \frac{[M^4]}{[M^2]^2} \right), \quad (10)$$

where $[\dots]$ is the “time” average. In the limit $\mathcal{N} \rightarrow \infty$, $g(\mu) = 0$ for $\mu < \mu_c$ and $g(\mu) = 1$ for $\mu > \mu_c$, hence $g(\mu)$ can be used to locate μ_c . As shown in Fig. 5, the Binder cumulant goes from zero to one as μ increases. The curves sharpen as \mathcal{N} increases, as an effect of the oscillations between positive and negative magnetization, which become less important as \mathcal{N} increases. From the largest \mathcal{N} we estimate

$$\begin{aligned} \mu_c^{BP} &= 0.743 \pm 0.005 \quad (z = 4) \\ \mu_c^{BP} &= 0.547 \pm 0.005 \quad (z = 6) \end{aligned}$$

which agrees with the above estimate from the average magnetization. We also verified that with these values of μ_c , the magnetization obeys $m_{BP} = a(\mu - \mu_c)^\beta$ for $\mu \simeq \mu_c$, with the mean-field exponent $\beta = 1/2$ and $a \simeq 0.23$.

Klein et al.⁴⁵ solved the BP recursion in the vicinity of μ_c using the mean random field approximation (MRF). Their results $\mu_c^{MRF} = 0.775$ ($z = 4$) and $\mu_c^{MRF} = 0.587$ ($z = 6$) (obtained after rescaling their value by an appropriate normalization factor \sqrt{z}) are slightly larger than our result μ_c^{BP} .

In order to obtain an estimate of μ_c from the finite- N branch-and-cut data, we computed the Binder cumulant $g(\mu, N)$, defined as in Eq.(10) but with the time average replaced by the sample average. According to finite-size scaling, the curves for $g(\mu, N)$ as a function of μ for various N must cross at the critical point $\mu = \mu_c$. In Fig. 6 we plot the Binder cumulant in the vicinity of the intersection point (note that the horizontal scale is much larger than that of Fig. 5), from which we obtain

$$\begin{aligned} \mu_c &= 0.77 \pm 0.02 \quad (z = 4) \\ \mu_c &= 0.56 \pm 0.02 \quad (z = 6). \end{aligned}$$

This agrees with μ_c^{BP} within the error bars, suggesting that also for the magnetization replica symmetry breaking corrections are small, causing a shift of μ_c of less than 3–4%. Replica symmetry breaking corrections are expected to increase with z . In the Sherrington-Kirkpatrick model (which is the $z \rightarrow \infty$ limit of the present model), corrections shift μ_c from 1.25 to 1. Although our numerical estimate of μ_c is slightly *larger* than μ_c^{BP} instead, this could be a statistical fluctuation or a finite size effect. The small size of replica symmetry breaking corrections to μ_c suggests that the mixed ferromagnetic spin-glass phase is narrow for these values of z , as also recently indicated for the three-dimensional Ising spin glass⁵¹.

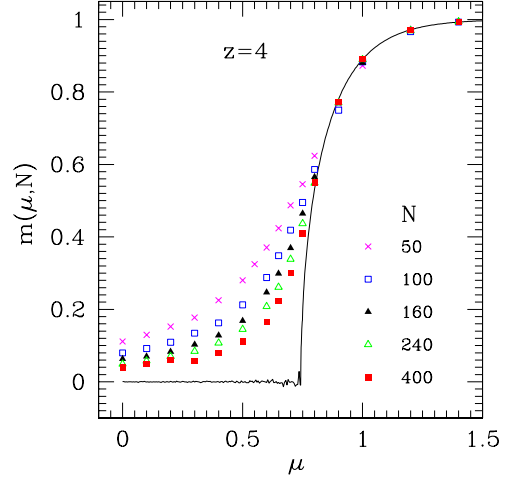


FIG. 3: Average ground-state magnetization as a function of the mean of the disorder distribution, μ , for $z = 4$. The symbols represent the results from the branch-and-cut algorithm, for various system sizes N . The statistical errors, not shown, are smaller than the symbol sizes. The line represents the numerical solution of the BP recursion, with a population size ranging from $\mathcal{N} = 10^3$ (away from the transition) to $\mathcal{N} = 10^5$ (near the transition), and with $\mathcal{M} = 10^4$ iterations of the stochastic algorithm.

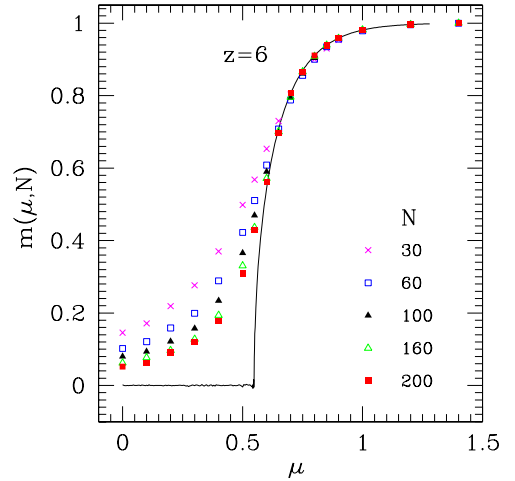


FIG. 4: Same as Fig. 3 but for $z = 6$.

The Binder cumulant is expected to satisfy the following finite-size scaling relation⁵² for $\mu \simeq \mu_c$:

$$g(\mu, N) = \tilde{g}(N^{1/(d_u \nu)}(\mu - \mu_c)) \quad (11)$$

where d_u is the upper critical dimension, which for the Ising spin glass is $d_u = 6$. As usual, by plotting $g(\mu, N)$ against $N^{1/(d_u \nu)}(\mu - \mu_c)$ with correct parameters μ_c and

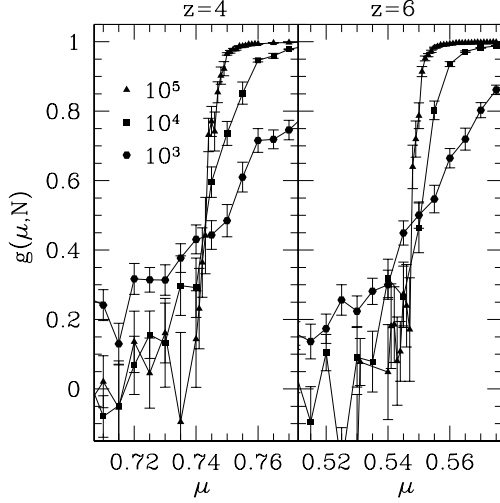


FIG. 5: Binder cumulant obtained by the iterative stochastic solution of the Bethe-Peierls ansatz, for three different sizes of the stochastic population $\mathcal{N} = 10^3, 10^4, 10^5$.

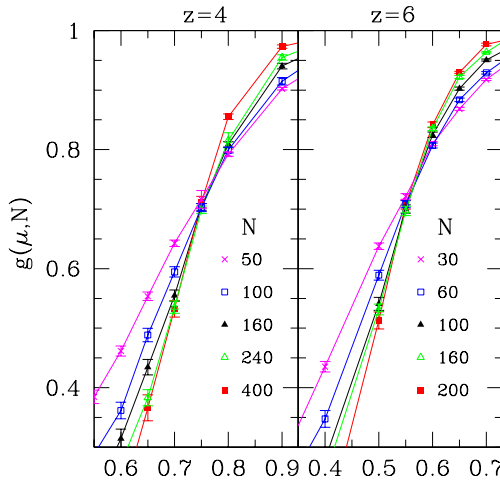


FIG. 6: Binder cumulant as a function of the mean of the disorder distribution, μ for various sizes. Left panel: connectivity $z = 4$. Right panel: connectivity $z = 6$. Only the region around the phase transition is shown.

ν , the data points for different system sizes should collapse onto a single curve near $(\mu - \mu_c) = 0$. As shown in Fig. 7, using the estimates of μ_c obtained above and the mean-field exponent $\nu = 1/2$ we obtain a good data collapse, showing that finite size scaling is well satisfied in our range of sizes.

In Fig. 8 we also show scaling plots for the average magnetization $m(\mu, N) = [M]_J$, whose scaling form is

$$m(\mu, N) = N^{-\beta/(d_u \nu)} \tilde{m}(N^{1/(d_u \nu)}(\mu - \mu_c)), \quad (12)$$

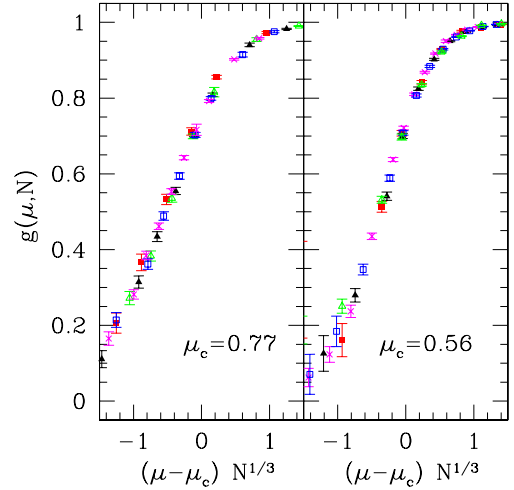


FIG. 7: Scaling plot for the Binder cumulant. The symbols for each panel are the same as the corresponding panels in Figure 6. The horizontal axis spans the same width in the two figures. Note that the scaling function for $z=6$ is has a steeper dependence on its argument.

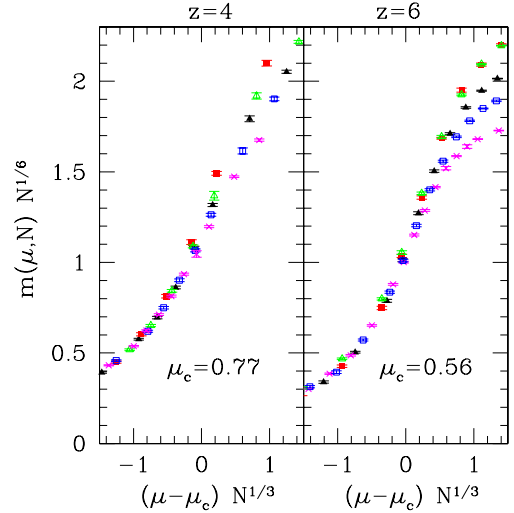


FIG. 8: Scaling plot for the ground state magnetization. The symbols for each panel are the same as those of Fig. 6. Note the significant corrections to scaling for $\mu > \mu_c$.

with the mean field exponent $\beta = 1/2$. The data show a good scaling collapse for $\mu \leq \mu_c$.

VI. TYPICAL RUNNING TIME OF OUR BRANCH AND CUT ALGORITHM

In this section we study the running time of our program as a function of the average coupling strength μ . In

computer science the complexity of a problem is classified in terms of the *worst-case* running time of its solution algorithms^{53,54}. Central notions here are the complexity classes P and NP. Informally, the class P consists of all *decision* problems (namely, problems whose solution can only be “yes” or “no”) for which at least one algorithm is known that can *generate* an answer in polynomial time, even in the “worst case”. The class NP consists of all decision problems for which, if for a given instance the answer is “yes”, then there is a *certificate* from which the correctness of the answer can be *verified* in polynomial time. For example, the question “Given a spin glass instance, is there a spin configuration with energy less than or equal to E_0 ?” belongs to NP. If for a given instance the answer is positive, then there is a spin configuration with correct energy, and its correctness can be verified in polynomial time. Here only the *existence* of such a certificate (spin configuration, in the above example) is required, we do not have to be able to *find* it in polynomial time. The class NP contains P, but it might be larger (many believe it is larger, and answering the question whether P = NP is an important open problem). NP-*complete* problems are the “most difficult” in the class NP, in the sense that no polynomial algorithm is known for solving them, and if a polynomial algorithm could be found for *one* of them, this would imply that *all* of them are polynomially solvable⁵⁵. The classes P and NP are defined for decision problems, but similar ideas apply to combinatorial optimization problems as well. Informally, an optimization problem is called NP-*hard*, if it is at least as difficult as every NP-complete problem. In particular, an optimization problem is NP-hard if the associated decision problem is NP-complete. This is true for many optimization problems, e.g. the maximum cut problem or the travelling salesman problem.

In practice, the running time can vary greatly from an instance of the problem to another, and the worst-case running time might very rarely occur. Recent work has therefore focused on the *average* (or average-case) running time, namely the average over the running times of random instances drawn from some probability distribution. Instead of the average one can also analyze the median, or *typical* running time. Calculating the typical running time has the advantage that the result is not influenced by the occurrence of exponentially rare samples with huge running times.

It should be noted that, unlike the worst-case complexity classification discussed above, which is an algorithm-independent feature of the problem itself, in general the typical running time can be different for different algorithms and implementations that solve the same problem.

Turning now to our problem, as mentioned in Section III, finding the ground state of the Bethe lattice spin glass is an NP-hard problem. For *all* values of μ the *possible* realizations of the disorder are the same as for $\mu = 0$. Hence, the algorithm has an exponential worst-case running time even on instances deep in the ferromagnetic phase. However, for large μ highly frustrated realizations

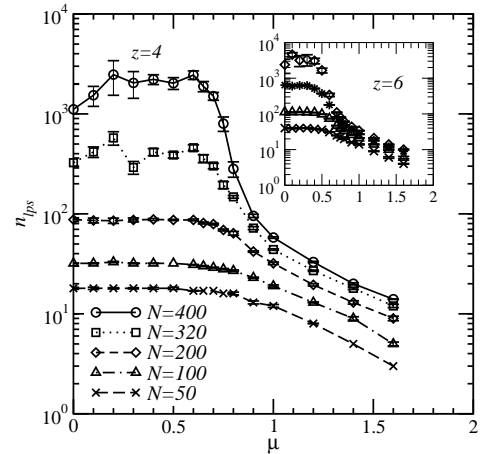


FIG. 9: Median running time (measured in number of solved linear problems) as a function of μ for different sizes $N = 400, 320, 200, 100, 50$ for $z = 4$. The inset shows the running time for $z = 6$ and system sizes $N = 200, 140, 100, 50$.

are very unlikely to appear, hence the *typical* running time will decrease as μ increases. The question we ask here is whether, for large N , the running time undergoes a *sharp* transition as a function of μ and, if so, whether the transition coincides with the spin-glass/ferromagnet phase transition.

One may use the CPU time as a measure of the running time. However, the CPU time is machine dependent, hence it is not suitable when different computers are used. Furthermore, it is hard to separate the influence of size-dependent hardware effects on the CPU time. In particular, small problems can be fully stored in the cache and therefore run faster. To avoid these problems, in the following we use the number of linear problems solved, n_{lps} , as a measure of the running time¹⁷.

In Fig. 9 we show the median running time as a function of μ for $z = 4, 6$ and different system sizes. Clearly (please note the logarithmic scale on the vertical axis) ground states are calculated quickly in the ferromagnetic region, while in the spin-glass phase the running time increases dramatically, and is approximately constant within the entire spin glass phase. The increase becomes more pronounced as N increases, suggesting a sharp discontinuity in the $N \rightarrow \infty$ limit around $\mu \approx 0.8$ ($z = 4$) and $\mu \approx 0.6$ ($z = 6$), which is close to the spin-glass/ferromagnetic transition μ_c .

As shown in Fig. 10, deep in the ferromagnetic phase the data is consistent with a polynomial increase of the running times. For smaller values of μ , the curves are bending upwards, indicating that the running time increases faster than any polynomial. This is also the case for $\mu = 0.8$ ($z = 4$) and for $\mu = 0.6$ ($z = 6$, not shown). Hence from this data, it seems that the change in the typical running time of our branch-and-cut algorithm occurs at a value of μ larger than μ_c for our distribution of instances, although it is difficult to locate a precise transi-

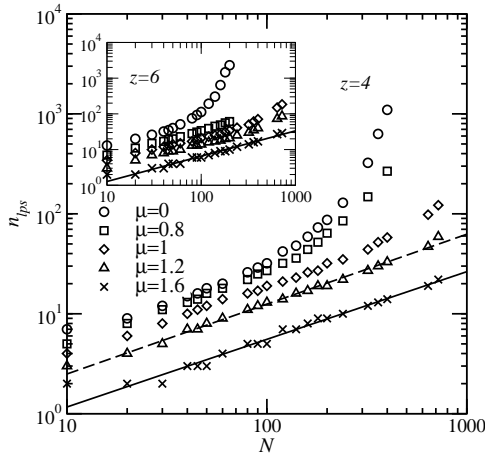


FIG. 10: Median running time (measured in number of solved linear problems) as a function of size N for different coupling strengths $\mu = 0, 0.8, 1, 1.2, 1.6$ in a log-log plot. The straight lines represent power-laws $c * N^\zeta$ with $\zeta = 0.699$ ($z = 4, \mu = 1.2$), $\zeta = 0.677$ ($z = 4, \mu = 1.6$) and $\zeta = 0.709$ ($z = 6, \mu = 1.6$), respectively, showing that in the ferromagnetic phase the median running time of our program is polynomial.

tion point. A similar mismatch between phase transition and change of the running time has been observed before, e.g. for a simple algorithm solving vertex cover¹³.

We have fitted the data in Fig. 10 with a function of the form $n_{lps}(N) \sim \exp(bN^c)$. For $\mu = 0$, we find $b = 0.026(9)$, $c = 0.87(5)$ for $z = 4$, and $b = 0.007(3)$ and $c = 1.24(8)$ for $z = 6$, but the data exhibits in both cases a considerable scatter around the fitting region, prohibiting to conclude in a definite way that the typical running time is exponential. Nevertheless, this data strongly suggests that in the spin-glass phase the typical running time is not polynomial.

VII. CONCLUSIONS

We have studied the ground state of a diluted mean-field Ising spin glass model with fixed connectivities $z = 4, 6$ and Gaussian distribution of the couplings, with mean μ and unit variance. We have applied a branch-and-cut algorithm, a sophisticated technique originating in combinatorial optimization which guarantees to find exact ground states. Our motivation was to study the ferromagnetic to spin-glass transition and relate it to the change in the typical running time of our algorithm.

From the study of the Binder-cumulant, we have ob-

tained values for the critical bond strength, μ_c . We have also solved the model in the Bethe-Peierls approximation, using an iterative stochastic procedure. In this approximation we obtain a critical bond strength, μ_c^{BP} , which agrees with the branch-and-cut estimate within the error bars of the latter, indicating that replica symmetry breaking effects are quantitatively small. Finite-size scaling is well satisfied for systems of size larger than $N \approx 30$.

We also analyzed the ground state energy, and found that the branch-and-cut results, extrapolated to the thermodynamic limit, are in very good agreement with the BP estimate, again indicating that replica symmetry breaking effects are quantitatively small. In the spin glass region, finite-size corrections are well described by a $N^{-2/3}$ dependence.

We investigated the typical running time of the branch-and-cut algorithm, which we defined as the median number of linear programs needed to find the ground state. We found that finding ground states is “hard” in the spin-glass phase and “easy” deep in the ferromagnetic region, with a sharp change occurring at a value of μ slightly larger than μ_c . More precisely, our implementation of the branch-and-cut method, which has an exponential worst-case running time, requires a superpolynomial number of steps in the spin-glass phase and a polynomial number of steps deep in the ferromagnetic region, on the computed instances. Although the running time of *one* special algorithm cannot be used to infer the “hardness” of the problem itself, it is reasonable to expect that the spin-glass/ferromagnet transition will manifest itself to some extent in the running time of many other solution algorithm.

Our understanding of what makes a problem computationally hard is still very weak. In this paper, we have shown that a standard problem from physics, the Ising spin glass, exhibits an easy-hard transition near a “physical” phase transition. We expect that similar phenomena can occur in other well known physical models.

Acknowledgments

We thank A.P. Young for comments on an earlier version of the paper, and the Regional Centre of Computing in Cologne for the allocation of computer time and various support. MP also thanks Alan Bray for a useful correspondence. AKH obtained financial support from the DFG (Deutsche Forschungsgemeinschaft) under grants Ha 3169/1-1 and Zi 209/6-1.

^{*} Electronic address: liers@informatik.uni-koeln.de

[†] Electronic address: matteo@maxwell.ucsf.edu

[‡] Electronic address: hartmann@theorie.physik.uni-goettingen.de

[§] Electronic address: mjuenger@informatik.uni-koeln.de

¹ B. Hayes, Amer. Scient. **85**, 108 (1997).

² R. Monasson, R. Zecchina, S. Kirkpatrick, B. Selman, and

L. Troyansky, Nature **400**, 133 (1999)

³ O. Dubois, R. Monasson, B. Selman, and R. Zecchina

⁴ (eds.), special issue of *Theor. Comp. Sci.* **265** (2001).

⁴ M.J. Alava, P.M. Duxbury, C.F. Moukarzel, H.Rieger, in *Phase transitions and critical phenomena, Vol. 18*, C. Domb and J. Lebowitz eds. (Academic Press, 2001).

⁵ A.K. Hartmann and H. Rieger, *Optimization Algorithms in Physics*, (While-VCH, Berlin 2001).

⁶ D. Mitchell, B. Selman, and H. Levesque, in Proc. 10th Natl. Conf. Artif. Intell. (AAAI-92), 440 (AAAI Press/MIT Press, Cambridge, Massachusetts, 1992).

⁷ R. Monasson, R. Zecchina, *Phys. Rev. E* **56**, 1357 (1997).

⁸ M. Weigt and A.K. Hartmann, *Phys. Rev. Lett.* **84**, 6118 (2000).

⁹ S. Mertens, *Phys. Rev. Lett.* **81**, 4281 (1998).

¹⁰ P. Cheeseman, B. Kanefsky, and W.M. Taylor, Proceedings of the Twelfth International Joint Conference on Artificial Intelligence, IJCAI-91, Sidney, Australia.

¹¹ In the computer science literature, the term *average-case running time* is usually employed.

¹² S. Cocco and R. Monasson, *Phys. Rev. Lett.* **86**, 1654 (2001).

¹³ M. Weigt and A.K. Hartmann, *Phys. Rev. Lett.* **86**, 1658 (2001).

¹⁴ F. Barahona, *J. Phys. A* **15**, 3241 (1982).

¹⁵ C. De Simone, M. Diehl, M. Jünger, P. Mutzel, G. Reinelt and G. Rinaldi, *J. Stat. Phys.* **84**, 1363 (1996)

¹⁶ A.K. Hartmann and A.P. Young, *Phys. Rev. B* **66**, 094419 (2002).

¹⁷ M. Palassini, F. Liers, M. Jünger, and A.P. Young, cond-mat/0212551.

¹⁸ A. Middleton, *Phys. Rev. Lett.* **88**, 017202 (2002).

¹⁹ M. Mézard and G. Parisi, *Eur. Phys. J. B* **20**, 217 (2001).

²⁰ M. Mézard and G. Parisi, cond-mat/0207121.

²¹ G. Parisi and F. Tria, cond-mat/0207144.

²² S. Boettcher, cond-mat/0208196.

²³ S. Franz and M. Leone, cond-mat/0208280.

²⁴ D.J. Thouless, *Phys. Rev. Lett.* **56** (1986) 1082.

²⁵ L. Viana and A.J. Bray, *J. Phys. C* **18**, 3037 (1985).

²⁶ P. Mottishaw, *Europhys. Lett.* **4** (1987) 333.

²⁷ D.J. Thouless, *Phys. Rev. Lett.* **56** (1986) 1082.

²⁸ P.Y. Lai and Y.Y. Goldschmidt, *J. Phys. A* **22**, 399 (1989).

²⁹ J.R. Banavar, D. Sherrington and N. Sourlas, *J. Phys. A* **20** L1 (1987).

³⁰ I. Bieche, R. Maynard, R. Rammal, and J.P. Uhry, *J. Phys. A* **13**, 2553 (1980).

³¹ L. Saul and M. Kardar, *Phys. Rev. E* **48**, R3221 (1993); *Nucl. Phys. B* **432**, 641 (1994).

³² A. Galluccio, M. Loebl, and J. Vondrák, *Math. Program. A*, **90**, 273 (2001).

³³ S. Kirkpatrick, C.D. Gelatt Jr. and M.P. Vecchi, *Science* **220**, 671 (1983).

³⁴ B. A. Berg and T. Celik, *Phys. Rev. Lett.* **69**, 2292 (1992).

³⁵ K.F. Pál, *Physica A* **233**, 60 (1996)

³⁶ M. Palassini and A.P. Young, *Phys. Rev. Lett.* **83**, 5126 (1999).

³⁷ J. Houdayer and O. C. Martin, *Phys. Rev. Lett.* **83**, 1030 (1999).

³⁸ A.K. Hartmann, *Phys. Rev. E* **59**, 84 (1999).

³⁹ C. De Simone, M. Diehl, M. Jünger, P. Mutzel, G. Reinelt and G. Rinaldi, *J. Stat. Phys.* **80**, 487 (1995).

⁴⁰ M. Jünger and D. Naddef eds., *Computational Combinatorial Optimization* (Lecture Notes in Computer Science 2241, Tutorial, Springer Verlag Heidelberg, 2001).

⁴¹ A. Hartwig, F. Daske and S. Kobe, *Comp. Phys. Commun.* **32** 133 (1984)

⁴² T. Klotz and S. Kobe, *J. Phys. A: Math. Gen.* **27**, L95 (1994).

⁴³ F. Barahona, M. Grötschel, M. Jünger, G. Reinelt, *Oper. Res.* **36**, 493 (1988).

⁴⁴ V. Chvátal, *Linear Programming* (Freeman, New York, 1983).

⁴⁵ Klein et al. *Phys. Rev. B* **19**, 1492 (1979).

⁴⁶ A. Steger and N.C. Wormald, *Combin. Probab. Comput.* **8** (1999), 377–396.

⁴⁷ M. Palassini, 2000, unpublished.

⁴⁸ A.K. Hartmann, from exact ground-state calculation of 2d spin glasses up to size $N = 480^2$ (unpublished)

⁴⁹ K. Binder, *Z. Phys. B* **43**, 119 (1981).

⁵⁰ For these values of μ , we restricted the average to the time intervals in which the magnetization is positive.

⁵¹ F. Krzakala and O.C. Martin, cond-mat/0208566.

⁵² V. Privman ed., *Finite Size Scaling and Numerical Simulation of Statistical Systems* (World Scientific, Singapore 1990).

⁵³ M.R. Garey and D.S. Johnson, *Computers and Intractability*, (Freeman, San Francisco, 1979).

⁵⁴ For an informal introduction to computational complexity for physicists, see S. Mertens, *Comp. Sci. Eng.* **4**, 31 (2002).

⁵⁵ For a treatment of complexity theory focussed on combinatorial optimization problems, see A. Ausiello, P. Crescenzi, G. Gambosi, V. Kann, A. Marchetti-Spaccamela, M. Protasi, *Complexity and Approximation*, Springer 1999.